
HYBRIDS OF CONSTRAINT-BASED AND NOISE-BASED ALGORITHMS FOR CAUSAL DISCOVERY FROM TIME SERIES

A PREPRINT

✉ **Charles K. Assaad***
EasyVista

✉ **Daria Bystrova***
Univ. of Grenoble Alpes, CNRS,
Univ. Savoie Mont Blanc, LECA
Inria, CNRS, Grenoble INP, LJK

✉ **Julyan Arbel**
Univ. of Grenoble Alpes, CNRS,
Inria, CNRS, Grenoble INP, LJK

✉ **Emilie Devijver**
Univ Grenoble Alpes,
CNRS, Grenoble INP, LIG

✉ **Eric Gaussier**
Univ Grenoble Alpes,
CNRS, Grenoble INP, LIG

✉ **Wilfried Thuiller**
Univ. of Grenoble Alpes, CNRS,
Univ. Savoie Mont Blanc, LECA

ABSTRACT

Constraint-based and noise-based methods have been proposed to discover summary causal graphs from observational time series under strong assumptions which can be violated or impossible to verify in real applications. Recently, a hybrid method [5] that combines these two approaches, proved to be robust to assumption violation. However, this method assumes that the summary causal graph is acyclic, but cycles are common in many applications. For example, in ecological communities, there may be cyclic relationships between predator and prey populations, creating feedback loops. Therefore, this paper presents two new frameworks for hybrids of constraint-based and noise-based methods that can discover summary causal graphs that may or may not contain cycles. For each framework, we provide two hybrid algorithms which are experimentally tested on simulated data, realistic ecological data, and real data from various applications. Experiments show that our hybrid approaches are robust and yield good results over most datasets.

Keywords Causal discovery · Time series · Noise-based · Constraint-based

1 Introduction

Recent technological advances allow collecting observational time series on complex dynamic systems in various fields, such as ecology, medical sciences, and IT systems. One of the key objectives in studying such dynamic systems is to understand the causal relationships between the system's components. However, in some applications, experts are not interested in understanding exact causal relations with the temporal lags between them. Instead, researchers rather opt for an abstract representation of the causal relationships between variables by using a summary causal graph [4], which provides an overview of the causal relationships between time series without delving into the details of their specific temporal relationships. To find these causal relations, experts can employ causal discovery methods for time series, which can be categorized into several families, including Granger [8], constraint-based [24, 20, 2] and noise-based families [11, 16] (for more details see [4]). Each family has its own set of assumptions, which may or may not be suitable for a specific dataset. Therefore, no single method stands out in all situations [4].

Recently, a hybrid method was proposed [5], which we denote as $\text{NBCB}^{\text{acyclic1}}$, that combines noise-based and constraint-based methods and shows that a hybrid approach can outperform non-hybrid approaches, especially when some assumptions are violated. However, $\text{NBCB}^{\text{acyclic}}$ assumes that the summary causal graph is acyclic, which is easily violated in many applications. For example, in ecological communities, there may be cyclic relationships be-

*These authors contributed equally to this work.

¹In [5], this method was called NBCB but in this work we denote it as $\text{NBCB}^{\text{acyclic}}$ to explicitly point out that it assumes that the summary causal graph is acyclic and we call our proposed framework as NBCB as it does not require the acyclicity assumption.

tween predator and prey populations, creating feedback loops. Therefore, building on NBCB^{acyclic}, this paper presents two new hybrid frameworks, NBCB (Noise-Based and Constraint-Based) and CBNB (Constraint-Based and Noise-Based), that can handle cyclic summary causal graphs. NBCB can be considered as a generalization of NBCB^{acyclic} and CBNB can be considered as a backward version of NBCB. Both frameworks start by inferring a type of causal graphs that differentiate between instantaneous relations and lagged relations and then deduce the summary causal graph from it. To construct these types of causal graphs, NBCB and CBNB orient edges using a restricted version of a noise-based algorithm and prune edges using a restricted version of a constraint-based algorithm. The main difference between NBCB and CBNB is that NBCB starts by orienting the graph and then proceeds to pruning, while CBNB starts by pruning and then proceeds to orientation. At the core of CBNB lies the notion of undirected cycle group which we introduce to optimize the search for orientation.

The remainder of the paper is organized as follows: Section 2 describes the different types of causal graphs that can be used to represent causal relations between time series as well as the different assumptions related to those graphs. Section 3 discusses related work. Section 4 introduces the two hybrid frameworks, NBCB and CBNB that can handle cyclic summary causal graphs. In Section 5, NBCB and CBNB are compared to different causal discovery algorithms on simulated, realistic and real datasets. Finally, Section 6 concludes the paper.

2 Causal graphs for time series

Causal relations in a dynamic system can be represented by a dynamic structural causal model (SCM) [15]. In this work, we assume that the dynamic SCM is linear and that there is no hidden common causes, i.e., causal sufficiency [24]. We will use the following dynamic SCM as running example:

$$\begin{aligned}
 X_t &:= a_x X_{t-1} + a_{yx} Y_t + a_{zx} Z_t + \xi_t^x \\
 Y_t &:= a_y Y_{t-1} + a_{xy} X_{t-1} + a_{wy} W_{t-2} + \xi_t^y \\
 Z_t &:= a_z Z_{t-1} + a_{xz} X_{t-1} + a_{yz} Y_t + a_{wz} W_{t-1} + \xi_t^z \\
 W_t &:= a_w W_{t-1} + a_{yw} Y_t + a_{zw} Z_t + \xi_t^w \\
 U_t &:= a_u U_{t-1} + a_{wu} W_t + \xi_t^u.
 \end{aligned} \tag{1}$$

Several causal graphs can be used to represent the causal relations of such a dynamic SCM qualitatively [4]. The most complete one is the full-time causal graph (Figure. 1a) which represents an infinite graph of the dynamic system through infinite nodes and infinite edges. The full-time causal graph is assumed to be acyclic and to satisfy the causal Markov condition, i.e., each node is independent of all other nodes, except for its descendants, given its parents [24]. Working with full-time causal graphs is often impractical, which has led to the adoption of simpler causal graphs, assuming that causal relations between time series hold throughout time. This is formalized in the following assumption, in which $\mathbf{V}^f = (\mathbf{V}_{t-\infty}, \dots, \mathbf{V}_t, \dots, \mathbf{V}_{t+\infty})$ where \mathbf{V} denotes a vector of d time series.

Assumption 1 (Consistency throughout time). *Let $G^f = (\mathbf{E}^f, \mathbf{V}^f)$ be a full-time causal graph. The graph G^f is said to be consistent throughout time if there exist γ in \mathbb{N}^* such that the causal structure of the graph consisting of the nodes $\{\mathbf{V}_{t-\gamma}, \dots, \mathbf{V}_t\}$ is the same for every t . We call the minimum value of γ for which the property holds, the maximal temporal lag of the graph.*

Under Assumption 1, the full-time causal graph is equivalent to the so-called window causal graph [11, 20] (Figure. 1b).

Definition 1 (Window causal graph, WCG). *Let $G^f = (\mathbf{E}^f, \mathbf{V}^f)$ be a full-time causal graph satisfying Assumption 1 with γ the maximal temporal lag in G^f . A window causal graph (WCG) $G^w = (\mathbf{E}^w, \mathbf{V}^w)$ is the subgraph of G^f consisting of the nodes $\mathbf{V}^w = (\mathbf{V}_{t-\gamma}, \dots, \mathbf{V}_t)$ and \mathbf{E}^w contains all related edges.*

Unfortunately, causal discovery methods still suffer in practice due to the strong assumptions (e.g., faithfulness [24]) they rely on that are not always satisfied. Thus, in many applications, experts have to validate those graphs before using them. However, validating WCGs is challenging for them: if they can usually identify causes and related effects, they do not know, in general, the exact temporal lags between them. For these reasons, it is easier to resort to abstractions of causal graphs. An extended summary causal graph [2] (Figure 1c) is one type of abstraction that can differentiate between instantaneous relations and lagged relations without giving precise information about the lag.

Definition 2 (Extended summary causal graph, ECG). *Let $G^w = (\mathbf{E}^w, \mathbf{V}^w)$ be a WCG with maximal temporal lag γ and nodes $(\mathbf{X}_{t-\gamma}, \dots, \mathbf{X}_t)$. The underlying extended summary causal graph (ECG) $G^e = (\mathbf{E}^e, \mathbf{V}^e)$ consists of the nodes $\mathbf{V}^e = (\mathbf{V}_{t-\gamma}, \mathbf{V}_t)$ and the set of directed edges \mathbf{E}^e is defined as follows: for all $X_t, Y_t \in \mathbf{V}_t$, $X_t \neq Y_t$, there exists a directed edge from X_t to Y_t (denoted as $X_t \rightarrow Y_t$) if and only if the same directed edge exists in G^w ; for all*

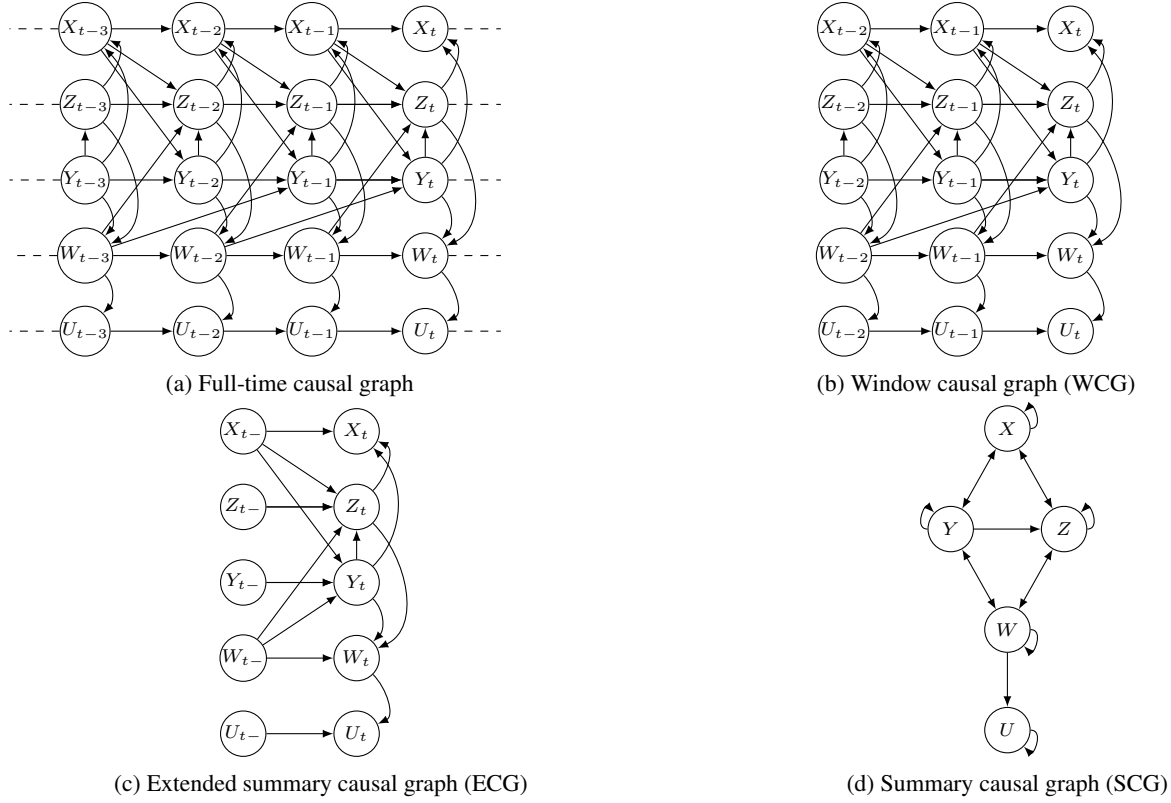


Figure 1: Different causal graphs to represent the dynamic SCM in (1): full time causal graph (1a), window causal graph (1b), extended summary causal graph (1c) and summary causal graph (1d).

$X_{t-} \in \mathbf{V}_{t-}, Y_t \in \mathbf{V}_t$, there exists a directed edge from X_{t-} to Y_t (denoted as $X_{t-} \rightarrow Y_t$) if and only if there exists at least one temporal lag $\ell > 0$ such that there exists a directed edge between $X_{t-\ell}$ and Y_t in G^w .

Another more abstract graphical representation is the summary causal graph [1, 16] (Figure 1d), where temporal information are completely omitted.

Definition 3 (Summary causal graph, SCG). Let $G^w = (\mathbf{E}^w, \mathbf{V}^w)$ be a WCG with maximal temporal lag γ . The underlying summary causal graph (SCG) of G^w is $G = (\mathbf{E}, \mathbf{V})$ where \mathbf{V} contains one node for each time series and the set of directed edges \mathbf{E} are defined as follows: for all $X, Y \in \mathbf{V}$, $X \neq Y$, there exists a directed edge from X to Y (denoted as $X \rightarrow Y$) if and only if there exists at least one temporal lag $\ell \geq 0$ such that there exists a directed edge between $X_{t-\ell}$ and Y_t in G^w .

Remark that because the full-time graph is supposed to be acyclic, the WCG and the ECG are also acyclic, but the SCG may be cyclic. For illustration, see the different causal graphs that can represent the running example in Figure 1.

3 Related works

Granger Causality is one of the oldest methods proposed to detect causal relations between time series. However, in its standard form [8], it is known to handle a restricted version of causality that focuses on linear relations and causal priorities as it assumes that the past of a cause is necessary and sufficient for optimally forecasting its effect. This approach has nevertheless been improved [9, 1] and can be used to infer a SCG assuming there is no instantaneous relations.

Noise-based approaches discover causal relations using footprints produced by the causal asymmetry in the data, namely the noise. For time series, one of the most popular algorithms in this family is VLiNGAM [11], which can discover the WCG assuming linear autoregressive models and non-Gaussian noise.

Constraint-based approaches [24] are certainly the most popular approaches for discovering causal graphs, and in case of causal sufficiency, they are usually based on the PC-algorithm [24]. PC-MCI⁺ [20] is an adaptation of the PC-algorithm to time series that can discover WCGs, and PCGCE [2] is an adaptation of the PC-algorithm that can discover ECGs. These approaches assume faithfulness which states that all conditional independencies are entailed from the causal Markov condition. In theory, a constraint-based algorithm can only infer a representative (known as a CPDAG [7]) of the Markov equivalence class [27] of the true WCG or the true ECG, i.e., the correct skeleton, the correct orientations for lagged relations, and all unshielded colliders [24] for instantaneous relation.

There also exist hybrid methods, which sometimes yield better results than non-hybrid methods. For example, [5] recently introduced a method, which we denote as NBCB^{acyclic}, that combines the noise-based and the constraint-based approaches to infer a SCG. However, this method assumes that the SCG is acyclic (with loops to represent self causes), which is considered an unrealistic assumption in many applications, for example, in ecology. Prior to NBCB, [10] presented a similar hybrid approach for non temporal data that starts with a constraint-based procedure to find the pattern of the graph and then uses a noise-based procedure to orient unoriented edges.

4 Hybrids of Constraint-based and Noise-based Algorithms

Here we present two hybrid frameworks, NBCB and CBNB, that can discover SCGs that may or may not contain cycles.

As NBCB^{acyclic} [5], NBCB and CBNB do not require the faithfulness assumption needed by the constraint-based family, instead, they need a weaker version of faithfulness, called adjacency faithfulness [19]².

Assumption 2 (Adjacency faithfulness). *Let $G^w = (E^w, V^w)$ For every $X_t, Y_{t'} \in V^w$ if $X_t \rightarrow Y_{t'}$ in E^w , then $\exists S \subseteq V^w \setminus \{X_t, Y_{t'}\}$ such that $X_t \perp\!\!\!\perp Y_{t'} \mid S$.*

In addition, similarly to the noise-based family, NBCB and CBNB require the following assumption, which guarantees the identifiability of the graph:

Assumption 3 (Identifiable functional model). *The data generating mechanism belongs to an identifiable functional model class as defined in [17].*

In this paper, we assume linear non-Gaussian models, but our methods can be extended to handle weaker identifiable functional model, such as additive noise models.

To overcome the acyclicity assumption of NBCB^{acyclic}, we start by inferring a WCG or an ECG and then deduce the SCG from it. As in NBCB^{acyclic}, we use a restricted version of a noise-based algorithm to orient edges and a restricted version of a constraint-based algorithm to prune edges.

4.1 Restricted version of a noise-based algorithm and restricted version of a constraint-based algorithm

A noise-based algorithm that infers a WCG relies on the fact that, under Assumption 3, a prediction model of a target node Y where the predictors are the true causes of Y should yield residuals (that represent the noise) that are independent of the causes. The procedure of such an algorithm can be divided into two main steps:

1. find the causal order between nodes by recursively performing regression and independence test between the predictors and residual (noise). The causal order is a list such that each node in the list cannot cause any node that precedes it in the list;
2. find which set of the predictors is not needed to keep the independence between other predictors and residuals. The former set of predictors is considered as not causally related to the node that is predicted and latter set of predictors are considered as the causes of this node.

In both frameworks, NBCB and CBNB, we use a restricted version of a given noise-based algorithm for time series. It is restricted in the sense that only step 1 is used and the causal order only includes instantaneous nodes V_t . For example, in Figure 1, the causal order of instantaneous nodes can either be $(Y_t, Z_t, X_t, W_t, U_t)$ or $(Y_t, Z_t, W_t, X_t, U_t)$. But note that even if only instantaneous nodes are accounted for, lagged nodes are used in the regression as means to account for confounder bias. For example, assuming linearity, we use the following regression model to compute the

²Under Faithfulness two nodes not adjacent in the graph are statistically independent only when conditioning on a set that is consistent with the causal Markov condition. However, under adjacency faithfulness the conditioning set is not necessarily consistent with the causal Markov condition.

residuals of each $Y_t \in \mathbf{V}_t$:

$$Y_t = \sum_{X_t \in \mathbf{V}_t \setminus \{Y_t\}} a_{xy} X_t + \sum_{Z_{t-\ell} \in \mathbf{V} \setminus \mathbf{V}_t} a_{zy\ell} Z_{t-\ell} + \xi_t^y. \quad (2)$$

Note that it is also possible to find the causal order only for a subset $\mathbf{I}_t \subset \mathbf{V}_t$ using only their parents in $\mathbf{P} \subseteq \mathbf{V} \setminus \mathbf{V}_t$ if every confounding bias of every two nodes $X_t, Y_t \in \mathbf{I}_t$ can be deconfounded using a subset of $\mathbf{P} \cup \mathbf{I}_t \setminus \{X_t, Y_t\}$ (this will be used for the CBNB framework). We call the restricted version of a noise-based algorithm as RestNB. We say that RestNB is consistent with Assumption 3 if it can theoretically yield the correct causal order from the data generated from a specific identifiable functional model. For example, we say that the restricted version of the VLiNGAM [11] is consistent with this assumption in case of linear non-Gaussian models.

On the other hand, a constraint-based algorithm for time series usually is an adaptation of the PC-algorithm[24] which was initially introduced for non-temporal data. It follows that most constraint-based algorithms for WCGs or ECGs can be divided into three main steps:

1. initialize a fully connected graph such that lagged relations are oriented using temporal priority (if $X_t - Y_{t'}$ and $t < t'$ then $X_t \rightarrow Y_{t'}$) and instantaneous relations are unoriented;
2. prune unnecessary edges using the following procedure:
 - (a) eliminate oriented or unoriented edges between nodes $(X_t, Y_{t'})$ if $X_t \perp\!\!\!\perp Y_{t'}$;
 - (b) for each pair of nodes $(X_t, Y_{t'})$ having an oriented or an unoriented edge between them, and for each subset of nodes $\mathbf{S} \subseteq \mathbf{V}^w \setminus \{X_t, Y_{t'}\}$ (resp. $\mathbf{S} \subseteq \mathbf{V}^e \setminus \{X_t, Y_{t'}\}$) of size $n = 1$ such that $\forall Z_{t''} \in \mathbf{S}$, $Z_{t''}$ is adjacent to X_t if $t'' = t$ or $Z_{t''}$ is a parent of X_t $t'' > t$, eliminate the edge between X_t and $Y_{t'}$ if $X_t \perp\!\!\!\perp Y_{t'} \mid \mathbf{S}$;
 - (c) iteratively repeat step (b) while increasing the size of the conditioning set n by 1 until there are no more adjacent pairs $(X_t, Y_{t'})$, such that there is a subset $\mathbf{S} \subseteq \mathbf{V}^e \setminus \{X_t, Y_{t'}\}$ of size n that that was not tested.
3. orient instantaneous relations using some Rules. These Rules are only valid when the faithfulness assumption is satisfied. For more details about these Rules in case of causal sufficiency, see [24, 13].

In both frameworks NBCB and CBNB, we use a restricted version of a given constraint-based algorithm for time series. It is restricted in the sense that only steps 1 and 2 are used. We call the restricted version RestCB and the output of such algorithm is a partially completed partially oriented WCG or ESG.

Definition 4 (Partially completed partially oriented WCG). *Let $G^w = (\mathbf{E}^w, \mathbf{V}^w)$ be a WCG. $G^{pw} = (\mathbf{E}^{pw}, \mathbf{V}^{pw})$ is a partially completed partially oriented WCG (PCPO-WCG) of G^w iff $\mathbf{V}^{pw} = \mathbf{V}^w$ and $\forall X_t, Y_{t'} \in \mathbf{V}^{pw}$, $X_t - Y_{t'} \in \mathbf{E}^{pw}$ iff $X_t \rightarrow Y_{t'} \in \mathbf{E}^w$ and $t = t'$, and $X_t \rightarrow Y_{t'} \in \mathbf{E}^{pw}$ iff $X_t \rightarrow Y_{t'} \in \mathbf{E}^w$ and $t \neq t'$.*

Definition 5 (Partially completed partially oriented ECG). *Let $G^e = (\mathbf{E}^e, \mathbf{V}^e)$ be an ECG. $G^{pe} = (\mathbf{E}^{pe}, \mathbf{V}^{pe})$ is a partially completed partially oriented ECG (PCPO-ECG) of G^e iff $\mathbf{V}^{pe} = \mathbf{V}^e$ and $\forall X_t, Y_t \in \mathbf{V}^{pe}$, $X_t - Y_t \in \mathbf{E}^{pe}$ iff $X_t \rightarrow Y_t \in \mathbf{E}^e$ and $\forall X_{t-}, Y_t \in \mathbf{V}^{pe}$, $X_{t-} \rightarrow Y_t \in \mathbf{E}^{pw}$ iff $X_{t-} \rightarrow Y_t \in \mathbf{E}^w$.*

In Figure 2 we provide an example of a PCPO-WCG and an example of a PCPO-ECG.

We also consider that RestCB has an option to take into account the causal order of the nodes, if this option is used then: step 1 would initialize a fully connected oriented graph as instantaneous relations can be oriented using the causal order, and step 2 would only search for $Z_{t'}$ that are parents of X_t .

The pseudo-codes of the abstract version of RestNB and RestCB are given respectively in Algorithms 1 and 2. To simplify notations, we use G^{we} for either a WCG or an ECG and we use G^{pwe} for either a POPC-WCG or a POPC-ECG. Here we presented a macro view of RestNB and RestCB, but in Supplementary Material, we provide one concrete algorithm of RestNB based on an existing noise-based algorithm and two concrete algorithms of RestCB based on existing causal discovery algorithms.

4.2 Noise-based followed by constraint-based and Constraint-based followed by Noise-based

Here we present NBCB, a generalization of NBCB^{acyclic} to SCGs that may or may not contain cycles by first constructing the corresponding WCG or the corresponding ECG. In the first part of NBCB, RestNB is used to find the causal order between all instantaneous nodes. Then in the second part, RestCB is used while taking into account the causal order as described in the previous section.

As far as we know, there exists no previous work that investigated the case where the constraint-based part of a hybrid method is executed before the noise-based part in causal discovery from time series. In theory, there is no clear

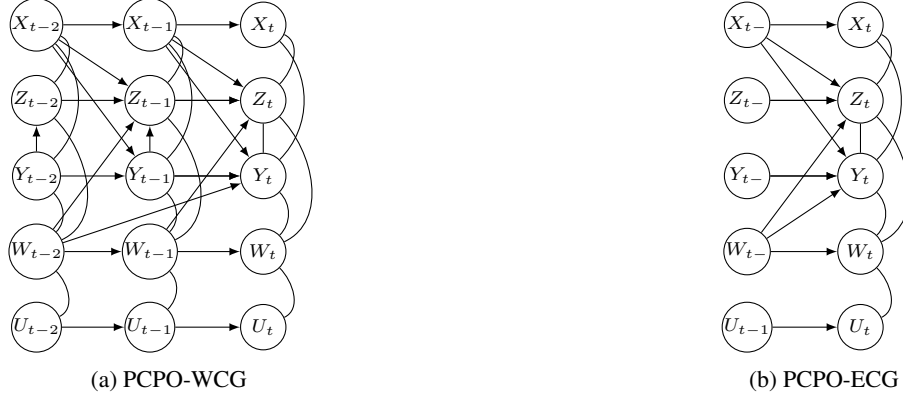


Figure 2: The PCPO-WCG (2a) corresponding to the WCG in Figure 1b and the PCPO-ECG (2b) corresponding to the ECG in Figure 1c.

argument why one part should be executed before the other. So here, we present a new frame called CBNB, where the constraint-based part is prior to the noise-based part.

In the first step of CBNB, RestCB is used to infer the PCPO-WCG or the PCPO-ECG. In the second step, a vanilla approach would be to apply RestNB over all instantaneous nodes (while taking into account of lagged common confounders), as it was done in NBCB, to get the causal order and then orient the instantaneous relations accordingly. However, we argue that this vanilla approach, despite being correct, is not optimal since it does not take into account the knowledge that had already been acquired through the construction of the PCPO-WCG or the PCPO-ECG. Therefore, we propose to apply RestNB over different groups of instantaneous nodes separately. To find these groups, we first need to define an undirected cycle path.

Definition 6 (Undirected cycle path). *In a PCPO-WCG $G^{\text{pw}} = (\mathbf{E}^{\text{pw}}, \mathbf{V}^{\text{pw}})$ (resp., PCPO-ECG $G^{\text{pe}} = (\mathbf{E}^{\text{pe}}, \mathbf{V}^{\text{pe}})$), a path $\pi = \langle X_t, Y_t, \dots, X_t \rangle$ is an undirected cycle path iff π is an undirected path in G^{pw} (resp., G^{pe}), only the first and last nodes of π are equal, and $\text{size}(\pi) \geq 3$.*

For example, in Figure 2a there is undirected cycle paths between X_t, Y_t, Z_t and between Z_t, Y_t, W_t , so $Z_t - Y_t$ would be in both cycles and would be considered twice, which is not only a computational problem, but it might also in practice induce bias. Thus, defining a cycle path alone is not sufficient. So, we combine all cycle paths that share at least one edge together in a cycle group³ which is defined as follows:

Definition 7 (Undirected cycle group). *In a PCPO-WCG $G^{\text{pw}} = (\mathbf{E}^{\text{pw}}, \mathbf{V}^{\text{pw}})$ (resp., PCPO-ECG $G^{\text{pe}} = (\mathbf{E}^{\text{pe}}, \mathbf{V}^{\text{pe}})$), \mathbf{C} is an undirected cycle group (UCG) of G^{pw} (resp., G^{pe}) iff \mathbf{C} is a set of undirected cycles and $\forall \pi_1, \pi_2 \in \mathbf{C}, \pi_1 \cap \pi_2 \neq \emptyset$.*

Given an UCG \mathbf{C} , we say that a node X_t belongs to \mathbf{C} iff $\exists \pi \in \mathbf{C}$ such that $X_t \in \pi$ and we say that an edge $X_t - Y_{t'}$ belongs to \mathbf{C} iff $\exists \pi \in \mathbf{C}$ such that $\langle X_t, Y_{t'} \rangle \in \pi$. In Figure 2a there are two UCGs, the first contains nodes X_t, Y_t, Z_t, W_t and the second contains nodes U_t, W_t . The same applies to Figure 2b.

Having brought out the concept UCG, we can now describe the second (noise-based) part of CBNB. Given a PCPO-WCG or a PCPO-ECG by the first part (constraint-based), CBNB searches for all UCGs. Then for each UCG \mathbf{C} , it applies RestNB between all nodes belonging to \mathbf{C} to find the causal order between these nodes. Using this causal order, it orients all edges belonging to \mathbf{C} . Finally, after having oriented all edges and obtained the WCG or the ECG, it deduces the SCG as in Definition 3.

Theorem 1. *Assuming causal sufficiency and Assumptions 1,2,3, and given a RestNB consistent with Assumption 3 and a RestCB for WCGs (resp. ECGs), NBCB and CBNB are guaranteed to find the correct WCGs (resp. ECGs) and the correct SCG from the joint distribution.*

The proof of Theorem 1 is available in Supplementary Material.

The pseudo-codes of NBCB and CBNB are respectively given in Algorithms 3 and 4. As before, to simplify notations, we use G^{we} for either a WCG or an ECG and we use G^{pwe} for either a POPC-WCG or a POPC-ECG. As one can see, NBCB and CBNB require a restricted version of a noise-based algorithm RestNB and a restricted version of a constraint-based algorithm RestCB.

³Note that our definition of cycle group is different than the one introduced in [23].

Algorithm 1: RestNB

Input: A multivariate time series, a maximal lag γ , a significance threshold α , an independence test $I()$, instantaneous nodes of interest $\mathbf{I}_t \subseteq \mathbf{V}_t$ and their past nodes $\mathbf{P} \subseteq \mathbf{P}^w \setminus \mathbf{V}_t$ such that $\mathbf{I}_t \cup \mathbf{P}$ satisfy causal sufficiency

Result: \mathbf{O} (causal order)

The details of the algorithm depend on the chosen noise-based algorithm.

Algorithm 2: RestCB

Input: A multivariate time series, a maximal lag γ and a significance threshold α , a conditional independence test $CI()$ and optionally a causal order \mathbf{O}

Result: \mathcal{G}^{we} (WCG) or \mathcal{G}^{pwe} (POPC-WCG)

The details of the algorithm depend on the chosen constraint-based algorithm.

Algorithm 3: NBCB

Input: A multivariate time series, a maximal lag γ and a significance threshold α , RestCB, RestNB, an independence test $I()$, and a conditional independence test $CI()$

Result: G^s (SCG) and G^{we} (WCG or ECG)

Find the causal order \mathbf{O} using RestNB (Algorithm 1) by setting \mathbf{I}_t to \mathbf{V}_t and \mathbf{P} to $\mathbf{V}^w \setminus \mathbf{V}_t$;

Discover the WCG or the ECG G^{we} using RestCB (Algorithm 2) given \mathbf{O} ;

Deduce the SCG G^s from G^{we} using Definition 3

Algorithm 4: CBNB

Input: A multivariate time series, a maximal lag γ and a significance threshold α , RestCB, RestNB, an independence test $I()$, and a conditional independence test $CI()$

Result: G^s (SCG) and G^{we} (WCG or ECG)

Discover the POPC-WCG or the POPC-ECG \mathcal{G}^{pwe} using RestCB (Algorithm 2);

for each UCG \mathbf{C} in \mathcal{G}^{pwe} do

\mathbf{V}_t^c : set of nodes that belong to \mathbf{C} ;

\mathbf{P}^c : Parents of \mathbf{V}_t^c in $\mathbf{V}^{pwe} \setminus \mathbf{V}_t$;

Find causal order \mathbf{O}^c between nodes in \mathbf{V}_t^c using RestNB (Algorithm 1) by setting \mathbf{I}_t to \mathbf{V}_t^c and \mathbf{P} to \mathbf{P}^c ;

Deduce the WCG or the ECG G^{we} using the order \mathbf{O} and G^{pwe} ;

Deduce the SCG G^s from G^w using Definition 3

5 Experiments

In this section, we propose first an extensive analysis⁴ on simulated data, generated from basic causal structures as well as on simulated but realistic benchmarks, and then, we perform an analysis on different real datasets.

5.1 Experimental setup

5.1.1 Baselines and hyper-parameters

We compare NBCB and CBNB with five state-of-the-art methods:

- the multivariate version of Granger Causality denoted GCMVL [1];
- the constraint-based methods PCMCI⁺ [20] for which we use the Python code available at <https://github.com/jakobrunge/tigramite> and PCGCE [2] for which the main Python code available at <https://github.com/ckassad/PCGCE> where we use the linear partial correlation to find conditional independencies and for PCGCE, as the authors suggested, we reduce the dimensionality of \mathbf{V}_{t-} in the ECG to 1 using PCA;

⁴The code of all our methods and of every experimentation is available in Supplementary Materials and will be rendered available online if the paper will be accepted.

Table 1: Structures of simulated data.

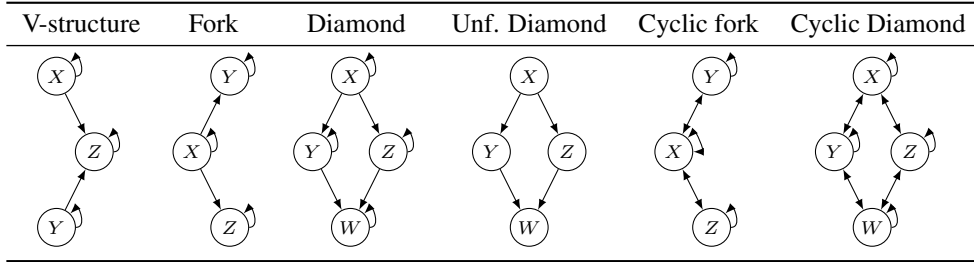


Table 2: Results obtained on the simulated data for the different structures with 1000 observations with non-Gaussian noise. We report the mean and the standard deviation of the F1 score. The best results are in bold.

	V-structure	Fork	Diamond	Unf. Diamond	Cyclic Fork	Cyclic Diamond
NBCB-w	0.92 ± 0.02	0.95 ± 0.01	0.94 ± 0.01	0.86 ± 0.01	0.83 ± 0.03	0.81 ± 0.01
CBNB-w	0.92 ± 0.03	0.96 ± 0.01	0.94 ± 0.01	0.9 ± 0.01	0.82 ± 0.03	0.8 ± 0.01
NBCB-e	0.77 ± 0.04	0.75 ± 0.05	0.74 ± 0.02	0.95 ± 0.01	0.75 ± 0.03	0.72 ± 0.01
CBNB-e	0.78 ± 0.05	0.76 ± 0.05	0.74 ± 0.02	0.96 ± 0.01	0.73 ± 0.02	0.7 ± 0.02
GCMVL	0.9 ± 0.02	0.9 ± 0.03	0.86 ± 0.01	0.04 ± 0.01	0.69 ± 0.01	0.68 ± 0.01
PCMCi ⁺	0.92 ± 0.02	0.94 ± 0.02	0.92 ± 0.01	0.47 ± 0.04	0.77 ± 0.03	0.75 ± 0.01
PCCGE	0.82 ± 0.03	0.75 ± 0.05	0.69 ± 0.02	0.5 ± 0.01	0.7 ± 0.02	0.66 ± 0.01
VLiNGAM	0.98 ± 0.01	0.98 ± 0.01	0.99 ± 0.01	0.98 ± 0.01	0.8 ± 0.04	0.8 ± 0.01

- the noise-based method VLiNGAM [11] for which we use the Python code available at <https://github.com/cdt15/lingam> where the regularization parameter in the adaptive Lasso is selected using BIC.

For all the methods, the maximal lag is set to $\gamma = 5$ and the significant threshold for hypothesis testing to 0.05. We test two versions of each of our frameworks. In the first version, which we denote as NBCB-w and CBNB-w, RestCB is based on the PCMCi⁺ algorithm, and in the second version, which we denote as NBCB-e and CBNB-e, RestCB is based on the PCGCE algorithm. In both versions, RestNB is based on the VLiNGAM algorithm. To find undirected cycle paths in CBNB-w and CBNB-e we use an adapted version of Paton’s algorithm [14].

5.1.2 Evaluation

In the different experimental settings, we compare the results with respect to the *F1-score* of the orientations in the SCG obtained without considering self causes, as it is treated differently depending on the methods. When there is more than one dataset, we report the mean and standard deviation for the F1 score.

5.2 Simulated data

The simulated datasets correspond to six causally sufficient SCGs presented in Table 1, extracted from WCGs, among which four are acyclic, one have correspond to an unfaithful distribution, and two are cyclic. The generating process of all datasets is the following: for all Y , for all $t > 0$,

$$Y_t = a_y Y_{t-1} + \sum_{X_{t-\ell} \in \text{Parents}(Y_t, G^w)} a_{xy} X_{t-\ell} + 0.1 \xi_t^y$$

where $a_y, a_{xy} \in U(-1, -0.1) \cup U(0.1, 1)$ and for each parent X we randomly choose if X causes Y instantaneously or with a lag of 1, i.e., $i \in \{0, 1\}$. Regarding the noise, we consider two different settings, in the first the noise is drawn from a uniform distribution, i.e., $\xi^y \sim U(-1, 1)$, and in the second the noise is drawn from a Gaussian distribution, i.e., $\xi^y \sim N(0, 1)$. For each setting and for each structure in Table 1 we generate 100 datasets of 1000 timestamps. For the unfaithful graph in Table 1, following [29], we set a_y to zero and $a^{yw} = -a^{xz} a^{zw} / a^{xy}$ and all relations are instantaneous.

In Table 2, we report the results for the setting with non-Gaussian noise. For the first three structures, VLiNGAM has the best performance, followed by NBCB-w, PCMCi⁺, and CBNB-w. Closest to these methods is GCMVL, whose F1 score is similar for V-structure and Fork but slightly declined in the case of the Diamond structure. For the Unfaithful

Table 3: Results obtained on the simulated data for the different structures with 1000 observations with Gaussian noise. We report the mean and the standard deviation of the F1 score. The best results are in bold.

	V-structure	Fork	Diamond	Unf. Diamond	Cyclic Fork	Cyclic Diamond
NBCB-w	0.83 ± 0.03	0.85 ± 0.04	0.78 ± 0.03	0.45 ± 0.06	0.81 ± 0.02	0.77 ± 0.01
CBNB-w	0.85 ± 0.01	0.84 ± 0.02	0.85 ± 0.01	0.45 ± 0.06	0.78 ± 0.02	0.75 ± 0.01
NBCB-e	0.7 ± 0.03	0.66 ± 0.05	0.64 ± 0.02	0.44 ± 0.07	0.71 ± 0.03	0.67 ± 0.02
CBNB-e	0.64 ± 0.05	0.66 ± 0.07	0.61 ± 0.04	0.45 ± 0.07	0.7 ± 0.03	0.65 ± 0.02
GCMVL	0.92 ± 0.02	0.91 ± 0.03	0.87 ± 0.01	0.02 ± 0.01	0.73 ± 0.02	0.7 ± 0.01
PCMCI ⁺	0.95 ± 0.01	0.94 ± 0.02	0.94 ± 0.01	0.42 ± 0.04	0.77 ± 0.03	0.75 ± 0.01
PCCGE	0.84 ± 0.04	0.77 ± 0.02	0.71 ± 0.01	0.5 ± 0.02	0.7 ± 0.03	0.65 ± 0.01
VLiNGAM	0.83 ± 0.04	0.86 ± 0.04	0.79 ± 0.04	0.43 ± 0.08	0.76 ± 0.03	0.74 ± 0.01

structure, also VLiNGAM performs best, followed by NBCB-e and then CBNB-e, followed by NBCB-w and CBNB-w. All other methods have lower performance. For cyclic structures, NBCB-w is the best, followed by VLiNGAM, CBNB-w, and PCMCI⁺.

In Table 3, we report the results for the setting with Gaussian noise. For the first three structures, PCMCI⁺ performs best, closely followed by GCMVL, CBNB-w and VLiNGAM, and slightly less performing NBCB-w and PCCGE. PCCGE has the best results for unfaithful structure, followed by NBCB-w, CBNB-w, CBNB-e, NBCB-e and VLiNGAM. Finally, for cyclic structures, NBCB-w has better results than the rest of the methods, followed by CBNB-w, PCMCI⁺ and VLiNGAM.

In sum, we can note that hybrid methods perform better than constraint-based methods when the faithfulness assumption is violated. At the same time, hybrid methods perform better than noise-based (VLiNGAM), when the assumption of non-Gaussianity of the noise is violated. Interestingly, for both types of noise, the hybrid methods have the best results for cyclic structures. Overall, the hybrid methods are more robust to different assumption violations.

5.3 Realistic data

We consider the simulation with multi-species generalization of the Ricker model introduced by [18], which is analogous to the generalized Lotka Volterra with abiotic control presented in the same paper and is commonly used in ecological studies. Ricker model with abiotic control in discrete time for abundance of species Y at time step t :

$$Y_t = \begin{cases} Y_{t-1} \exp \left(\Delta t \left(\sum_{X_{t-1} \in \text{Parents}(Y_t, G^w)} a_{xy} X_{t-1} + \bar{Y} (-a_y) \exp \left(-\frac{(o_y - x)^2}{2\sigma_y^2} \right) \right) + \epsilon_t^y \right) & \text{preys} \\ Y_{t-1} \exp \left(\Delta t \left(\sum_{X_{t-1} \in \text{Parents}(Y_t, G^w)} a_{xy} X_{t-1} - \mu \right) + \epsilon_t^y \right), & \text{predators} \end{cases}$$

where Y_t is the abundance of species Y at time t and the upper equation is related to preys and the lower to predator species, \bar{Y} is the abundance of species Y in the stationary state, a_{xy} is the strength of the effect of species X on species Y and a_y is strength of the effect of species Y on itself, ϵ_t^y is an i.i.d Gaussian random variable with variance σ_r , o_y is a niche optimum for species Y , x is the environmental variable, μ is the extinction rate of the predator. We run this simulation for the number of species $S = \{5, 10\}$ with the following fixed parameters: fixed environment $x = 0.5$, number of time steps $T = 1000$, $\mu = 0.05$, $\sigma_r = 0.2$ randomly assign o_y for each species between 0 and 1, the interaction matrix related to coefficients a_{xy} and a_y is obtained through randomly generated graph G , such that G has 3 trophic levels and G is connected graph (for more details see [18]). All links in this graph are bi-directed, and the interactions strength is randomly sampled for all interactions.

On this data, NBCB-w performs better than the other methods followed by CBNB-w as it is shown in Table 5. Close to them perform CBNB-e, PCCGE and PCMCI⁺. GCMVL has the lowest result.

5.4 Real data

Four different real datasets are considered in this study. We detail the performance of each method in the following paragraphs, but the results⁵ are summarized in the last four columns of Table 5.

Temperature. This bivariate time series, available at <https://webdav.tuebingen.mpg.de/cause-effect/>, of length 168 is about indoor I and outdoor O measurements. As noted by [5], it is expected that O causes I .

⁵The results we obtained for VLiNGAM on the temperature and on the Dairy datasets are different than the results reported in [5].

Table 4: Results for realistic datasets generated using the Lotka Volterra model where number of species is in parenthesis. We report the mean and the standard deviation of the F1 score.

	Lotka Volterra(5)	Lotka Volterra(10)
NBCB-w	0.4 \pm 0.03	0.26 \pm 0.01
CBNB-w	0.34 \pm 0.04	0.24 \pm 0.01
NBCB-e	0.4 \pm 0.02	0.19 \pm 0.01
CBNB-e	0.36 \pm 0.03	0.21 \pm 0.01
GCMVL	0.21 \pm 0.03	0.13 \pm 0.01
PCMCI ⁺	0.33 \pm 0.04	0.21 \pm 0.01
PCGCE	0.36 \pm 0.03	0.2 \pm 0.01
VLiNGAM	0.22 \pm 0.06	0.22 \pm 0.02

Table 5: Results for real datasets. We report the mean and the standard deviation of the F1 score.

	Temperature	Veilleux	Dairy	Ingestion mini	Web	Antivirus
NBCB-w	1	0.5 \pm 0.25	0.4	0.47 \pm 0.03	0.2	0.13
CBNB-w	1	0.5 \pm 0.25	0.4	0.46 \pm 0.11	0.23	0.18
NBCB-e	1	1 \pm 0.0	0.4	0.5 \pm 0.05	0.24	0.29
CBNB-e	1	1 \pm 0.0	0.4	0.52 \pm 0.06	0.15	0.33
GCMVL	0.67	1 \pm 0.0	0.33	0.5 \pm 0.03	0.19	0.08
PCMCI ⁺	1	0.5 \pm 0.25	0.4	0.3 \pm 0.08	0.17	0.04
PCGCE	1	1 \pm 0.0	0.4	0.55 \pm 0.03	0.21	0.3
VLiNGAM	1	1 \pm 0.0	0.5	0.49 \pm 0.05	0.23	0.18

NBCB-w, CBNB-w, NBCB-e, CBNB-e, PCMCI⁺, PCGCE, and VLiNGAM correctly infer $O \rightarrow I$. GCMVL infers a bidirected causal relation.

Veilleux. We considered two datasets available at <http://robjhyndman.com/tsdldata/data/veilleux.dat>, datasets for Figure 11(a) and 12(a) [12] from [26] which study interactions between predatory ciliate *Dinidium nasutum* and its prey *Paramecium aurelia* with different values of Cerophyl concentrations (CC): 0.375 and 0.5. The lengths of the time series are 71 and 65. These data were previously analyzed with causal discovery algorithms [6, 25], which showed bidirectional relationships in both cases.

Here, NBCB-e, CBNB-e, GCMVL, PCGCE and VLiNGAM discover bidirected relationships *Paramecium* \leftrightarrow *Dinidium* in both datasets, which is consistent with [25, 6]. CBNB-w, NBCB-w, PCMCI⁺ have detected bidirected relationships between *Paramecium* and *Didinium* only in the first dataset.

Diary. This dataset, available at <http://future.aae.wisc.edu>, provides ten years (from 09/2008 to 12/2018) of monthly prices for milk M , butter B , and cheddar cheese C , so the three time series are of length 124. We expect that the price of milk is a common cause of the price of butter and the price of cheddar cheese: $B \leftarrow M \rightarrow C$.

NBCB-w, CBNB-w, NBCB-e, CBNB-e, PCMCI⁺, PCGCE and VLiNGAM correctly inferred that $M \rightarrow B$. But NBCB-w and CBNB-w wrongly inferred that $M \leftarrow C \rightarrow B$, NBCB-e, CBNB-e, wrongly inferred that $M \leftarrow B \leftarrow C$, PCMCI⁺ and PCGCE wrongly inferred that $M \leftarrow C \leftarrow B$, and VLiNGAM wrongly inferred that $C \rightarrow B$. Granger wrongly infers $B \leftrightarrow M \leftarrow C \rightarrow B$.

Ingestion mini. This benchmark consists of 24 datasets each containing 3 time series with 1000 timestamp collected from an IT monitoring system with a one minute sampling rate. It is provided by EasyVista and available at https://easyvista2015-my.sharepoint.com/personal/aait-bachir_easyvista_com/_layouts/15/onedrive.aspx?id=%2Fpersonal%2Faait%2Dbachir%5Feasyvista%5Fcom%2FDocuments%2FLab%2FPublicData&ga=1. Half the datasets are compatible with the graph $C.M.I \leftarrow M.E \rightarrow G.H.I$ [3] where $M.E$ is the metric extraction which represents the activity of the extraction of the metrics from the messages; $G.H.I$ is the group history insertion, which represents the activity of the insertion of the historical status in the database; and $C.M.I$ is the collector monitoring information, which represents the activity of the updates in a given database. The second half of the datasets are compatible with the graph $M.D \rightarrow M.E \rightarrow M.I$ where $M.D$ is the metric dispatcher which represents the activity of a process that orient messages to other process with respect to different types of messages; and $M.I$ is the metric insertion which represents the activity of insertion of data in a database. Lags between time series are unknown, as well as the existence of self-causes.

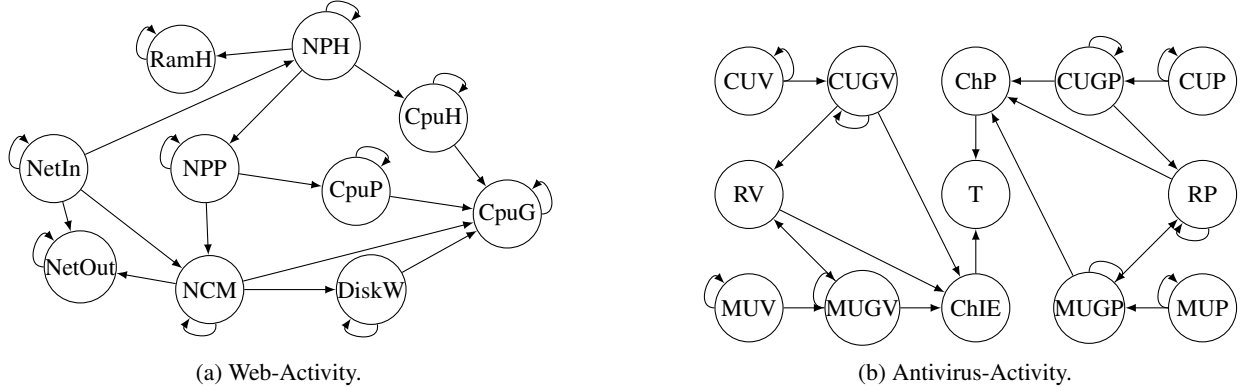


Figure 3: Summary causal graphs for the Web activity dataset (a) and the Antivirus activity dataset (b). Those summary causal graphs are constructed by an IT monitoring system’s experts.

From Table 5, we can see that PCGCE have the best results followed by CBNB-e then by NBCB-e and GCMVL. After that comes NBCB-w and CBNB-w. Finally, PCMCI⁺ has the worst result. This might suggest that the lags between causes an effects are not consistent over time, in the sense that if the lags between two time series varies (while respecting the maximum lag), the extended summary causal graph might remain the same however this is not true for the window causal graph. In this case, we might expect that methods inferring window causal graphs (such as PCMCI⁺) would perform worst than methods inferring extended summary causal graph (as PCGCE).

Web This dataset consists of 10 time series which represent a web activity and were collected using an IT monitoring system. Initially, these time series had a 1 minute sampling rate and they were misaligned. Therefore, they were resampled each 5 minutes and different data points were temporally aligned according to the closest point in time. After pre-processing the dataset contains 2500 timestamps. The summary causal graph which represents the causal relations between these time series is given in Figure 3a. NetIn represents the network in Kbytes/second; NPH represents the number of HTTP processes; NPP represents the number of PHP processes; NCM represents the number of open MySql connections; NetOut represents the network out Kbytes/second; CpuH represents the CPU used by the HTTP process; RamH represents the RAM used by the HTTP process; CpuP represents the CPU used by the PHP process; DiskW represents the disk write; CpuG represents the global CPU usage.

From Table 5, we can see that NBCB-e demonstrates the highest performance, followed by CBNB-w and VLiNGAM. Next are PCGCE, NBCB-w and GCMVL. CBNB-e exhibits the lowest score.

Antivirus. This dataset consists of 11 time series which represent an antivirus activity and were collected using an IT monitoring system. Initially these time series were misaligned and some of them had a 1 minute sampling rate and others had a 5 minute sampling rate. Therefore, we resample them with a 5 minutes and different data points were temporally aligned according to their closest point in time. After pre-processing the dataset contains 1321 timestamps. The summary causal graph which represents the causal relations between these time series is given in Figure 3b. CUV represents the CPU usage of antivirus processes in server V; MUV represents the Memory usage of antivirus process in server V; RV represents the Disk IO read in server V; CUGV presents the global CPU in server V; MUGV represents the global RAM in server V; ChIE represents the required duration to open an IE browser on server V; CUP represents the CPU usage of antivirus processes in server P; MUP represents the Memory usage of antivirus process in server P; RP represents the Disk IO read in server P; CUGP presents the global CPU in server P; MUGP represents the global RAM in server P; ChP represents the required duration to open a CITRIX Portal on server P; T represents the global time required to open a CITRIX portal and open the IE browser.

From Table 5, we can see that CBNB-e achieves the best result followed by PCGCE and NBCB-e and then by CBNB-w, VLiNGAM and NBCB-w. GCMVL and PCMCI⁺ have low performance, with PCMCI⁺ being the worst.

Notice that for all results in Table 5, NBCB-w and CBNB-w (which are based on a restricted versions of PCMCI⁺ and VLiNGAM) never perform simultaneously worst than PCMCI⁺ and VLiNGAM. Similarly, NBCB-e and CBNB-e (which are based on a restricted versions of PCGCE and VLiNGAM) never perform simultaneously worst than PCGCE and VLiNGAM, except for the Web dataset where CBNB-e has the lowest F1-score (but NBCB-e has the best F1-score). And in general, NBCB-e and CBNB-e seems to be more reliable than NBCB-w and CBNB-w for the real data we considered. However, it seems that there is no significance difference in performance between NBCB and CBNB when they are based on the same algorithms.

6 Conclusion

In this paper, we introduced two frameworks for hybrids of noise-based and constraint-based methods that can discover summary causal graphs that may or may not contain cycles. For each framework we proposed two algorithms that were experimentally compared with known causal discovery algorithms on toy simulated data, on realistic ecological data, as well as on real data from various domains. Overall, the performance of our algorithms is a trade-off between the performance of constraint-based and noise-based algorithms.

For future work, it would also be interesting to use a nonlinear conditional independence test and a nonlinear regression model as well as to adapt those algorithms for the case where consistency throughout time or stationarity are violated. It would also be interesting to adapt these methods for mixed data, this adaptation is straightforward in the case for the constraint-based part of our algorithms as there exists conditional independence test for mixed data [28]. However it is more challenging for the noise-based part.

References

- [1] Andrew Arnold, Yan Liu, and Naoki Abe. Temporal causal modeling with graphical granger methods. In *Proceedings of the 13th ACM SIGKDD International Conference on Knowledge Discovery and Data Mining*, KDD '07, page 66–75, New York, NY, USA, 2007. Association for Computing Machinery.
- [2] Charles K. Assaad, Emilie Devijver, and Eric Gaussier. Discovery of extended summary graphs in time series. In James Cussens and Kun Zhang, editors, *Proceedings of the Thirty-Eighth Conference on Uncertainty in Artificial Intelligence*, volume 180 of *Proceedings of Machine Learning Research*, pages 96–106. PMLR, 01–05 Aug 2022.
- [3] Charles K. Assaad, Emilie Devijver, and Eric Gaussier. Entropy-based discovery of summary causal graphs in time series. *Entropy*, 24(8), 2022.
- [4] Charles K. Assaad, Emilie Devijver, and Eric Gaussier. Survey and evaluation of causal discovery methods for time series. *J. Artif. Int. Res.*, 73, may 2022.
- [5] Charles K. Assaad, Emilie Devijver, Eric Gaussier, and Ali Ait-Bachir. A mixed noise and constraint-based approach to causal inference in time series. In *Machine Learning and Knowledge Discovery in Databases. Research Track*, pages 453–468, Cham, 2021. Springer International Publishing.
- [6] Frédéric Barraquand, Coralie Picoche, Matteo Detto, and Florian Hartig. Inferring species interactions using granger causality and convergent cross mapping. *Theoretical Ecology*, 14(1):87–105, 2021.
- [7] David Maxwell Chickering. Learning equivalence classes of bayesian-network structures. *J. Mach. Learn. Res.*, 2:445–498, mar 2002.
- [8] Clive Granger. Investigating causal relations by econometric models and cross-spectral methods. *Econometrica*, 37(3):424–38, 1969.
- [9] Clive W. J. Granger. Time series analysis, cointegration, and applications. *The American Economic Review*, 94(3):421–425, 2004.
- [10] Patrik O. Hoyer, Aapo Hyvärinen, Richard Scheines, Peter L. Spirtes, Joseph Ramsey, Gustavo Lacerda, and Shohei Shimizu. Causal discovery of linear acyclic models with arbitrary distributions. In *Conference on Uncertainty in Artificial Intelligence*, 2008.
- [11] Aapo Hyvärinen, Shohei Shimizu, and Patrik O. Hoyer. Causal modelling combining instantaneous and lagged effects: An identifiable model based on non-gaussianity. In *Proceedings of the 25th International Conference on Machine Learning*, ICML '08, pages 424–431, New York, NY, USA, 2008. ACM.
- [12] Christian Jost and Stephen P Ellner. Testing for predator dependence in predator-prey dynamics: a non-parametric approach. *Proceedings of the Royal Society of London. Series B: Biological Sciences*, 267(1453):1611–1620, 2000.
- [13] Christopher Meek. Causal inference and causal explanation with background knowledge. In *Proceedings of the Eleventh Conference on Uncertainty in Artificial Intelligence*, UAI'95, page 403–410, San Francisco, CA, USA, 1995. Morgan Kaufmann Publishers Inc.
- [14] Keith Paton. An algorithm for finding a fundamental set of cycles of a graph. *Commun. ACM*, 12(9):514–518, sep 1969.
- [15] Judea Pearl. *Causality: Models, Reasoning, and Inference*. Cambridge University Press, New York, NY, USA, 2000.

- [16] Jonas Peters, Dominik Janzing, and Bernhard Schölkopf. Causal inference on time series using restricted structural equation models. In *Advances in Neural Information Processing Systems 26*, pages 154–162, 2013.
- [17] Jonas Peters, Joris M. Mooij, Dominik Janzing, and Bernhard Schölkopf. Identifiability of causal graphs using functional models. In *Proceedings of the Twenty-Seventh Conference on Uncertainty in Artificial Intelligence*, UAI'11, page 589–598, Arlington, Virginia, USA, 2011. AUAI Press.
- [18] Giovanni Poggiato, Jérémy Andréoletti, Laura Shirley, and Wilfried Thuiller. Integrating food webs in species distribution models improves ecological niche estimation and predictions. nov 2022.
- [19] Joseph Ramsey, Peter Spirtes, and Jiji Zhang. Adjacency-faithfulness and conservative causal inference. In *Proceedings of the Twenty-Second Conference on Uncertainty in Artificial Intelligence*, UAI'06, page 401–408, Arlington, Virginia, USA, 2006. AUAI Press.
- [20] Jakob Runge. Discovering contemporaneous and lagged causal relations in autocorrelated nonlinear time series datasets. In Jonas Peters and David Sontag, editors, *Proceedings of the 36th Conference on Uncertainty in Artificial Intelligence (UAI)*, volume 124 of *Proceedings of Machine Learning Research*, pages 1388–1397. PMLR, 03–06 Aug 2020.
- [21] Shohei Shimizu, Patrik O. Hoyer, Aapo Hyvärinen, and Antti Kerminen. A linear non-gaussian acyclic model for causal discovery. *Journal of Machine Learning Research*, 7(72):2003–2030, 2006.
- [22] Shohei Shimizu, Takanori Inazumi, Yasuhiro Sogawa, Aapo Hyvärinen, Yoshinobu Kawahara, Takashi Washio, Patrik O. Hoyer, and Kenneth Bollen. Directlingam: A direct method for learning a linear non-gaussian structural equation model. *Journal of Machine Learning Research*, 12(33):1225–1248, 2011.
- [23] Peter Spirtes. Directed cyclic graphical representations of feedback models. In *Proceedings of the Eleventh Conference on Uncertainty in Artificial Intelligence*, UAI'95, page 491–498, San Francisco, CA, USA, 1995. Morgan Kaufmann Publishers Inc.
- [24] Peter Spirtes, Clark Glymour, and Richard Scheines. *Causation, Prediction, and Search*. MIT press, 2nd edition, 2000.
- [25] George Sugihara, Robert May, Hao Ye, Chih hao Hsieh, Ethan Deyle, Michael Fogarty, and Stephan Munch. Detecting causality in complex ecosystems. *Science*, 338(6106):496–500, 2012.
- [26] BG Veilleux. An analysis of the predatory interaction between paramecium and didinium. *The Journal of Animal Ecology*, pages 787–803, 1979.
- [27] Thomas Verma and Judea Pearl. Equivalence and synthesis of causal models. In *Proceedings of the Sixth Annual Conference on Uncertainty in Artificial Intelligence*, UAI '90, page 255–270, USA, 1990. Elsevier Science Inc.
- [28] Lei Zan, Anouar Meynaoui, Charles K. Assaad, Emilie Devijver, and Eric Gaussier. A conditional mutual information estimator for mixed data and an associated conditional independence test. *Entropy*, 24(9), 2022.
- [29] Zhalama, J. Zhang, and W. Mayer. Weakening faithfulness: some heuristic causal discovery algorithms. *International Journal of Data Science and Analytics*, 3:93–104, 2016.

A Proofs

We also recall the definition of blocked paths, backdoor paths, and the backdoor criterion. Formally, the blocked path is defined as follows:

Definition 8 (Blocked path, [15]). *A path is said to be blocked by a set of nodes $\mathbf{S} \subset \mathbf{V}$ if it contains an intermediate cause or a common cause X such that $X \in \mathbf{S}$ and if it contains a collider X such that $X \notin \mathbf{S}$ and no descendant of X is in \mathbf{S} .*

Definition 9 (Backdoor path, [15]). *A path between an ordered pair (X, Y) is said to be a blocked path between X and Y if it contains an arrow into X .*

Note that blocking all backdoor path between two nodes eliminate confounding bias [15].

In the following, we provide the proof of Theorem 1.

Proof. In the first part, we prove Theorem 1 for NBCB, and in the second part, for CBNB.

(1) This proof is similar to the proof of Theorem 4 in [5] for NCBN⁰. Given the Assumption 3 and causal sufficiency and assuming RestNB is consistent with Assumption 3, RestNB (Algorithm 1) would infer the correct causal order \mathbf{O} . Given the causal ordering \mathbf{O} and temporal priority, we can orient all edges in a fully-connected graph, which represents a super graph that contains the true graph. Given the causal Markov condition and assumptions 2, 1 and assuming that the CB algorithm on which RestCB is based is sound and complete, if we do not consider the causal order, RestCB (Algorithm 2) would prune all unnecessary edges by removing edges between two nodes that are conditionally independent given a subset \mathbf{S} adjacent to these two nodes and yield the correct skeleton. Given the causal order \mathbf{O} , the subset \mathbf{S} can be reduced by containing only parents (instead of adjacencies). Thus, again by the causal Markov condition and causal sufficiency, removing all edges between the conditionally independent nodes, the only edges that we will be left with are causal, and so the graph would be correct.

(2) Now, we prove Theorem 1 for CBNB. Without any given causal order, RestCB uses the first two steps of the constraint-based algorithm (omitting the orientation step). Using the full constraint-based algorithm under the assumptions of causal Markov condition and causal sufficiency in addition to the faithfulness assumption (which we do not really assume), we would obtain the Markov equivalence class of WCG or ESG represented by a CPDAG. In our case, using RestCB, it is obvious that under the same assumptions but by replacing faithfulness with adjacency faithfulness, we obtain the true partially complete partially oriented (PCPO) WCG or ESG, i.e., true skeleton, all instantaneous relations are not oriented and all lagged relations are oriented. So, having the PCPO-WCG or PCPO-ECG, what is left to prove is that applying RestNB (Algorithm 1) on the nodes \mathbf{V}_t^c of each cyclic group given the past parents \mathbf{P}^c is free of confounding bias. To obtain the correct causal order \mathbf{O}^c between nodes \mathbf{V}_t^c , we need to verify that in the subgraph of the nodes \mathbf{V}_t^c (which is by definition acyclic) for every two adjacent nodes $X_t, Y_t \in \mathbf{V}_t^c$, there exists set $\mathbf{S} \subseteq \mathbf{V}_t^c \setminus \{X_t, Y_t\} \cup \mathbf{P}^c$, such that \mathbf{S} blocks all backdoor paths between X_t and Y_t (if there is no edge between nodes X_t and Y_t , then there is no orientation to be determined by RestNB). Suppose $X_t \rightarrow Y_t$ in the true graph (but in the PCPO-WCG or PCPO-ECG this edge is unoriented) and there exists some backdoor path π between X_t and Y_t , we consider two cases:

(a) Suppose all nodes in path π belong to \mathbf{V}_t^c . In this case, any backdoor path π between X_t and Y_t can be blocked by any node on the path. By definition of an undirected cyclic group \mathbf{C} , all these nodes are in \mathbf{V}_t^c , which means that the common cause (common ancestor) on the path is also in \mathbf{V}_t^c , i.e., causal sufficiency is satisfied. Thus the $\exists \mathbf{S} \subseteq \mathbf{V}_t^c \setminus \{X_t, Y_t\}$ such that all backdoor paths between X_t and Y_t are blocked.

(b) Suppose that some nodes in π belong to \mathbf{P}^c . In this case, conditioning on \mathbf{P}^c blocks any backdoor path between X_t and Y_t since \mathbf{P}^c are the parents of \mathbf{V}_t^c and none of the nodes in \mathbf{P}^c are colliders of any two nodes in \mathbf{V}_t^c . So all the backdoor paths that are left are the ones discussed in (a).

□

B Pseudo-code algorithms

In our experimental section, we used a restricted version of the VLiNGAM algorithm, which we denote as RestVLiNGAM, and we used respectively a restricted version of the PCMCI⁺ algorithm, which we denote as RestPCMCI⁺ and a restricted version of the PCGCE algorithm which we denote as RestPCGCE. In the following, we provide the pseudo-codes of all restricted algorithms that we used. But first, we start by briefly recalling VLiNGAM, PCMCI⁺, and PCGCE algorithms which all assume causal sufficiency.

VLiNGAM [11] is a noise-based causal discovery algorithm for time series data that constructs a WCG. First, it estimates a classic autoregressive model for the data using any conventional implementation of a least-squares method. It then computes the residuals and then performs the LiNGAM analysis [21, 22] on the residuals. Note that the LiNGAM analysis can be either done using the ICALiNGAM [21] or DirectLiNGAM [22], in this work, we use DirectLiNGAM. This gives the causal order and the estimate of the instantaneous causal effects. After that, it computes the estimates of lagged causal effects. Finally, it estimates redundant directed edges to find the underlying WCG.

PCMCI⁺ [20] is a constraint-based causal discovery algorithm for time series data that constructs a WCG. First, the PC1 lagged phase infers a superset of the lagged parents together with the parents of instantaneous ancestors. Next, the MCI instantaneous phase starts with links found in the previous step and all possible instantaneous links, then it conducts momentary conditional independence (MCI) with a modified conditioning set learned in the previous step to increase detection power. Finally, it orients edges using the same Rules used in the PC algorithms [24, 13].

Similarly, PCGCE [2] is also a constraint-based causal discovery algorithm for time series data, but that constructs an ECG without passing by a WCG. It also consists of two steps. First, it searches for the skeleton of the ECG using a procedure similar to the PC-algorithm that is order independent by using a conditional independence test between either two nodes in the present slice or one node in the present slice and one node in the past slice, which can be multidimensional. Then it orients edges using the same Rules used in the PC algorithms [24, 13].

In the following, we present the restricted algorithms that we used in the experimental section. We color in blue the parts that are different from the initial algorithms. Remark that these blue parts indicates that these part are added or modified with respect to the initial algorithms, but they do not indicate parts of the initial algorithms that were deleted in the restricted versions.

B.1 RestVLiNGAM

RestVLiNGAM is a restricted version of VLiNGAM, which is almost identical to the DirectLiNGAM algorithm. The main difference between RestVLiNGAM and DirectLiNGAM is that, as VLiNGAM, RestVLiNGAM starts by computing the residuals of all instantaneous nodes by regressing them on their past. In addition, unlike DirectLiNGAM and VLiNGAM, RestLiNGAM can focus only on a subset of instantaneous nodes $\mathbf{I}_t \subseteq \mathbf{V}_t$ if a subset $\mathbf{P} \subseteq \mathbf{V}^w \setminus \mathbf{V}_t$ is provided such that $\mathbf{I}_t \cup \mathbf{P}$ satisfy causal sufficiency. The pseudo-code of RestVLiNGAM is provided in Algorithm 5.

B.2 RestPCMCI⁺

RestPCMCI⁺ is a restricted version of the PCMCI⁺ algorithm, which uses conditional independence test CI() that returns at the same time the p-value and the statistic of the test. To simplify notations, in the following, we will denote both WCG and POPC-WCG as G^w . The main difference with PCMCI⁺ is that RestPCMCI⁺ can optionally take a causal order as input, and in case the causal order is given it starts with a fully-connected graph, and in the MCI instantaneous phase, it conditions only using parents (PCMCI⁺ condition also on instantaneous adjacencies). In addition, RestPCMCI⁺ does not include the orientation phase that is used in PCMCI⁺. The pseudo-code of RestPCMCI⁺ is provided in Algorithm 6.

B.3 RestPCGCE

RestPCGCE is a restricted version of the PCGCE algorithm which uses conditional independence test CI() that returns either the p-value of the test or the statistic without computing the p-value. Again to simplify notations, in the following, we will denote both ECG and POPC-ECG as G^e . The main difference with PCGCE is that RestPCGCE can optionally take a causal order as input, and in case the causal order is given it starts with a fully-connected graph and it conditions only using parents (PCGCE condition on adjacencies). In addition, RestPCGCE does not include the orientation phase that is used in PCGCE. The pseudo-code of RestPCGCE is provided in Algorithm 7.

Algorithm 5: RestVLiNGAM

Input: A multivariate time series, a maximal lag γ , a significance threshold α , an independence test $I()$, instantaneous nodes of interest $\mathbf{I}_t \subseteq \mathbf{V}_t$ and their past nodes $\mathbf{P} \subseteq \mathbf{P}^w \setminus \mathbf{V}_t$ such that $\mathbf{I}_t \cup \mathbf{P}$ satisfy causal sufficiency

Result: \mathbf{O} (causal order)

for $Y_t \in \mathbf{I}_t$ **do**

Estimate a classic autoregressive model for the data

$$Y_t = \sum_{X_{t-\ell} \in \mathbf{P}} a_{xy\ell} X_{t-\ell} + \xi_t^y$$

using any conventional implementation of a least-squares method. Note that here $\ell > 0$, so it is really a classic AR model;

Compute the residuals, that is, estimates of ξ_t^y ;

$$\hat{\xi}_t^y = Y_t - \sum_{X_{t-\ell} \in \mathbf{P}} \hat{a}_{xy\ell} X_{t-\ell}$$

Initialize an empty order list \mathbf{O} ;

Initialize a list \mathbf{S} containing all nodes in \mathbf{I}_t ;

while $\text{size}(\mathbf{S}) > 0$ **do**

Initialize an empty list \mathbf{H} ;

for $X_t \in \mathbf{S}$ **do**

for $Y_t \in \mathbf{S} \setminus \{X_t\}$ **do**

Perform least squares regressions of $\hat{\xi}_t^x$ on $\hat{\xi}_t^y$ and compute the residuals:

$$\hat{\epsilon}^{Y_t} = \hat{\xi}_t^y - \frac{\text{cov}(\hat{\xi}_t^x, \hat{\xi}_t^y)}{\text{var}(\hat{\xi}_t^x)}$$

Estimate the dependence between the total residuals and X_t :

$$h = \sum_{Y_t \in \mathbf{S} \setminus \{X_t\}} I(\hat{\xi}_t^x, \hat{\epsilon}^{Y_t})$$

Append h to the end of \mathbf{H} ;

Find the node X_t corresponding to $\hat{\xi}_t^x$ that is most independent of its residuals;

Append X_t to the end of \mathbf{O} ;

Remove X_t from \mathbf{S} ;

Append the remaining instantaneous node to the end of \mathbf{O} .

Algorithm 6: RestPCMCI⁺

Input: A multivariate time series, a maximal lag γ and a significance threshold α , a conditional independence test $CI()$ and **optionally a causal order \mathbf{O}**

Result: \mathcal{G}^w (WCG or POPC-WCG)

if \mathbf{O} is given then

Construct an fully-connected WCG $\mathcal{G}^w = (\mathbf{E}^w, \mathbf{V}^w = \{\mathbf{V}_{t-}, \mathbf{V}_t\})$ such that
 $\forall X_{t-} \in V_{t-}, Y_t \in V_t, X_{t-} \rightarrow Y_t \in \mathbf{E}^w$ and $\forall X_t, Y_t \in V_t$ such that $X_t \neq Y_t, X_t \rightarrow Y_t \in \mathbf{E}^w$ if X_t precedes Y_t in the causal order \mathbf{O} ;
 Initialize $GET(Y_t, G^w)$ as a function to search for parents of Y_t in G^w ;

else

Construct a fully-connected POPC-WCG $\mathcal{G}^w = (\mathbf{E}^w, \mathbf{V}^w = \{\mathbf{V}_{t-}, \mathbf{V}_t\})$ such that
 $\forall X_{t-} \in V_{t-}, Y_t \in V_t, X_{t-} \rightarrow Y_t \in \mathbf{E}^w$ and $\forall X_t, Y_t \in V_t$ such that $X_t \neq Y_t, X_t - Y_t \in \mathbf{E}^w$;
 Initialize $GET(Y_t, G^w)$ as a function to search for adjacencies of Y_t in G^w ;

for $Y_t \in \mathbf{V}_t$ do

Initialize $\hat{B}_t(Y_t) = \mathbf{V}^w \setminus \mathbf{V}_t$;
 Initialize $I^{\min}(X_{t-\ell}, Y_t) = \infty \forall X_{t-\ell} \in \hat{B}_t(Y_t)$;
 $n = 0$;
while $\exists X_{t-\ell} \in \hat{B}_t(Y_t)$ s.t. $\text{size}(\hat{B}_t(Y_t)) \geq n$ **do**
 for $X_{t-\ell} \in \mathbf{V}^w \setminus \mathbf{V}_t$ s.t. $\text{size}(\hat{B}_t(Y_t)) \geq n$ **do**
 $\mathbf{S} =$ first n nodes in $\hat{B}_t(Y_t)$;
 $p, h = CI(X_{t-\ell}, Y_t \mid \mathbf{S})$;
 $I^{\min}(X_{t-\ell}, Y_t) = \min(|h|, I^{\min}(X_{t-\ell}, Y_t))$;
 if $p > \alpha$ **then**
 mark $X_{t-\ell}$ for removal
 $\forall X_{t-\ell}$ marked for removal, remove $X_{t-\ell} \rightarrow Y_t$ from \mathbf{E}^w ;
 Sort $\hat{B}_t(Y_t)$ by $I^{\min}(X_{t-\ell}, Y_t)$ from largest to smallest;
 $n = n + 1$;

Initialize $I^{\min}(X_{t-\ell}, Y_t) = \infty \forall X_{t-\ell} \in \hat{B}_t(Y_t)$;

$n = 0$;

while $\exists X_{t-\ell} - Y_t \in \mathbf{E}^w \forall \ell \geq 0$ s.t. $\text{size}(GET(Y_t, G^w) \cap \mathbf{V}_t \setminus \{X_{t-\ell}\}) \geq n$ **do**

for $X_{t-\ell} - Y_t \in \mathbf{E}^w \forall \ell \geq 0$ s.t. $\text{size}(GET(Y_t, G^w) \cap \mathbf{V}_t \setminus \{X_{t-\ell}\}) \geq n$ **do**
 while $\exists X_{t-\ell} - Y_t \in \mathbf{E}^w$ and not all $\mathbf{S} \in GET(Y_t, G^w) \cap \mathbf{V}_t \setminus \{X_{t-\ell}\}$ with $\text{size}(\mathbf{S}) = n$ have been considered **do**
 for $\mathbf{S} \in GET(Y_t, G^w) \cap \mathbf{V}_t \setminus \{X_{t-\ell}\}$ s.t. $\text{size}(\mathbf{S}) = n$ **do**
 $p, h = CI(Y_t, X_{t-\ell} \mid \mathbf{S}, \hat{B}_t(Y_t) \setminus \{X_{t-\ell}\}, \hat{B}_{t-\ell}(X_{t-\ell}))$;
 $I^{\min}(X_{t-\ell}, Y_t) = \min(|h|, I^{\min}(X_{t-\ell}, Y_t))$;
 if $p > \alpha$ **then**
 Remove $X_{t-\ell} \rightarrow Y_t$ from \mathbf{E}^w or $X_{t-\ell} - Y_t$ from \mathbf{E}^w ;
 $n = n + 1$;

Sort $GET(Y_t, G^w) \cap \mathbf{V}_t$ by $I^{\min}(X_{t-\ell}, Y_t)$ from largest to smallest;

Algorithm 7: RestPCGCE

Input: A multivariate time series, a maximal lag γ and a significance threshold α , a conditional independence test CI() and optionally a causal order \mathbf{O}

Result: \mathcal{G}^e (ECG or POPC-ECG)

if \mathbf{O} is given **then**

Construct an fully-connected ECG $\mathcal{G}^e = (\mathbf{E}^e, \mathbf{V}^e = \{\mathbf{V}_{t-}, \mathbf{V}_t\})$ such that
 $\forall X_{t-} \in V_{t-}, Y_t \in V_t, X_{t-} \rightarrow Y_t \in \mathbf{E}^e$ and $\forall X_t, Y_t \in V_t$ such that $X_t \neq Y_t, X_t \rightarrow Y_t \in \mathbf{E}^e$ if X_t precedes Y_t in the causal order \mathbf{O} ;
 Initialize GET(Y_t, G^e) as a function to search for parents of Y_t in G^e ;

else

Construct a fully-connected POPC-ECG $\mathcal{G}^e = (\mathbf{E}^e, \mathbf{V}^e = \{\mathbf{V}_{t-}, \mathbf{V}_t\})$ such that
 $\forall X_{t-} \in V_{t-}, Y_t \in V_t, X_{t-} \rightarrow Y_t \in \mathbf{E}^e$ and $\forall X_t, Y_t \in V_t$ such that $X_t \neq Y_t, X_t - Y_t \in \mathbf{E}^e$;
 Initialize GET(Y_t, G^e) as a function to search for adjacencies of Y_t in G^e ;

$n = 0$;

while $\exists X_{t*} - Y_t \in \mathbf{E}^e \forall t* \in \{t, t-\}$ s.t. $\text{size}(\text{GET}(Y_t, G^e) \setminus \{X_{t*}\}) \geq n$ **do**

Initialize \mathbf{D} as empty an list and \mathbf{P} and \mathbf{H} as empty dictionaries;

for $X_{t*} - Y_t \in \mathbf{E}^e \forall t* \in \{t, t-\}$ s.t. $\text{size}(\text{GET}(Y_t, G^e) \setminus \{X_{t*}\}) = n$ **do**

while $\exists X_{t*} - Y_t \in \mathbf{E}^e$ and not all $\mathbf{S} \in \text{GET}(Y_t, G^e) \setminus \{X_{t*}\}$ with $\text{size}(\mathbf{S}) = n$ have been considered **do**

for $\mathbf{S} \subset \text{GET}(Y_t, G^e) \setminus \{X_{t*}\}$ s.t. $\text{size}(\mathbf{S}) = n$ **do**

$-, h = \text{CI}(X_{t*}, Y_t \mid \mathbf{S})$;

Save $X_{t*}, Y_t \mid \mathbf{S}$ in \mathbf{D} and h in $\mathbf{H}(X_{t*}, Y_t, \mathbf{S})$

Sort \mathbf{D} and \mathbf{H} by \mathbf{H} from smallest to largest;

for $X_{t*}, Y_t, \mathbf{S} \in \mathbf{D}$ s.t. $\mathbf{S} \subseteq \text{GET}(Y_t, G^e)$ **do**

$p, - = \text{CI}(X_{t*}, Y_t \mid \mathbf{S})$;

if $p > \alpha$ **then**

Remove $X_{t*} \rightarrow Y_t$ from \mathbf{E}^e or $X_{t*} - Y_t$ from \mathbf{E}^e ;

$n = n + 1$;